



HAL
open science

Embedded printed magnetic needle probes sensor for the real-time control of the local induction state through a laminated magnetic core

Sorelle Hilary Nguedjang Kouakeuo, Y.A. Tena Deffo, B. Ducharne, Laurent Morel, M.A. Raulet, P. Tsafack, J.M. Garcia-Bravo, B. Newell

► To cite this version:

Sorelle Hilary Nguedjang Kouakeuo, Y.A. Tena Deffo, B. Ducharne, Laurent Morel, M.A. Raulet, et al.. Embedded printed magnetic needle probes sensor for the real-time control of the local induction state through a laminated magnetic core. *Journal of Magnetism and Magnetic Materials*, 2020, 505, pp.166767. 10.1016/j.jmmm.2020.166767 . hal-02559888

HAL Id: hal-02559888

<https://hal.science/hal-02559888>

Submitted on 22 Aug 2022

HAL is a multi-disciplinary open access archive for the deposit and dissemination of scientific research documents, whether they are published or not. The documents may come from teaching and research institutions in France or abroad, or from public or private research centers.

L'archive ouverte pluridisciplinaire **HAL**, est destinée au dépôt et à la diffusion de documents scientifiques de niveau recherche, publiés ou non, émanant des établissements d'enseignement et de recherche français ou étrangers, des laboratoires publics ou privés.



Distributed under a Creative Commons Attribution - NonCommercial 4.0 International License

Embedded printed magnetic needle probes sensor for the real-time control of the local induction state through a laminated magnetic core.

S.H. Nguedjang Kouakeuo^{1,2,3}, Y.A. Tena Deffo^{1,2}, B. Ducharne², L. Morel³, M.A. Raulet³, P. Tsafack¹, J. M. Garcia-Bravo⁴, B. Newell⁴.

¹Faculty of Engineering and Technology, University of Buea, Buea, Cameroon

²Laboratoire de Génie Electrique et Ferroélectricité, INSA de Lyon, 69100 Villeurbanne, France.

³Laboratoire Ampère, Université de Lyon, 69621 Villeurbanne, France

⁴School of Engineering Technology, Purdue University, West Lafayette, IN, 47907 USA.

Abstract

The magnetic needle probe method is a technique used to locally measure the magnetic state of a magnetic component. This concept has a rich conceptual history, but it has rarely been used in the industrial field. There are mainly two reasons for this: instrumentation limitations and inappropriate sizes of sensors' geometries. The first limitation has been overcome recently due to large improvements in both the analog and digital electronic fields. In this study, the second limitation, size/geometry is addressed by printing the magnetic needle probe using conductive ink directly on the ferromagnetic element to be controlled. The resulting sensor exhibits a drastic volume reduction. Such improvements allow measurement of the magnetic state of a previously inaccessible magnetic lamination through a magnetic laminated core. This opens up the possibility of measuring in situ magnetic behavior and monitoring many electromagnetic devices such as electric transformers, AC/DC electric motors, or even real-time electromagnetic non-destructive testing of ferromagnetic steel components. Over the past few years, simulation approaches including space discretization methods: finite elements, finite differences, and boundary elements have been proposed to describe the internal behavior of magnetic lamination stacks but experimental results validating these simulations could not be realized due to the aforementioned limitations. The printed magnetic needle probe method (PMNPM) described in this paper can be used to collect such local information and to validate homogenization methods. Experimental validations are proposed by comparing the sum of the laminations magnetic induction, they are individually measured with the PMNPM method to calculate the average induction obtained from a surrounding coil.

Keywords

Needle probe method, magnetic induction sensor, laminated magnetic core, conductive ink, printed sensor

I - Introduction

A laminated magnetic core is composed of a large number of stacked magnetic sheets. Magnetic materials are characterized by high permeability and reduced magnetic losses. These materials are used to confine and to conduct magnetic fields in almost all modern electromagnetic devices, examples include electromagnets, electric transformers, and electric motors [1]. Magnetic cores are made out of ferromagnetic materials such as iron based alloys. Magnetic cores are generally made from magnetic lamination stack-ups. Some high frequency applications do use ferrite magnetic cores as well, but the majority of applications use magnetic lamination stacks [2]. The large permeability difference between the magnetic material and the surrounding air ($\mu_{CM} \gg \mu_{air}$) forces the magnetic flux to be restrained inside the magnetic core. The magnetic field source can have different origins (permanent magnets, current densities, among others) but the usual excitation source for a magnetic core comes from a current-carrying coil of wires surrounding the structure. **Using a magnetic core can increase the strength of a magnetic field in an electromagnetic coil by a factor of several hundred times compared to the strength without the core.** However, magnetic cores have side effects that one has to consider before creating a new electromagnetic device. One of them is the magnetic energy losses which emerge under alternating magnetic excitation. Magnetic hysteresis and eddy currents are the main causes of these magnetic losses. Reducing these losses is of major interest, but to be successful in meeting this goal, an understanding of what is going on inside these laminations is required. For the last few decades, researchers from all around the world have been working on this topic and using simulation tools to predict this behavior [3]-[4].

The Electric steel market is vast and includes lamination steel, silicon electrical steel, silicon steel, relay steel and transformer steel. It is expected to exceed 39 billion by 2023 [5]. An estimation of the world's magnetic losses is not available but power losses in the distribution and transmission of electricity are. For example, in 2014 an average of approximately 8 % of the electrical energy produced was lost between the producer and the consumer [6]. A large amount of this energy was lost during voltage level conversions in magnetic transformers through hysteresis and eddy current losses. Improving such

conversions is, with no doubt, of major interest. Many options exist to gain a better efficiency from this energy conversion including enhancing the material magnetic properties. Anisotropic grain-oriented electric steel provides an example of an improved material. Laminated cores, made of stacks of silicon steel thin sheets is another option which is particularly efficient to reduce losses from macroscopic eddy currents. Each electric steel layer is coated to maximize the electrical resistance between laminations, while also providing resistance to corrosion and lubrication during die cutting. Different types of coatings exist, including organic and inorganic. The coating used depends on the application of the lamination [7] and on the heat and metallurgic treatment of the electric steel. Historically, early practices included insulating each magnetic lamination with a layer of paper, but this technique reduced the stacking factor and the maximum working temperature so is generally avoided in current production.

Stacking and coating the magnetic laminations, design improvements and increasing the homogeneity of the magnetic circuit have led to improvements in the efficiency of magnetic conversion.

Going forward with this improvement process, it is fundamental to have access to the distribution of the magnetic fields in the stack-up via sensors. Current magnetic sensors and experimental setups are limited to cross-section averaged information or limited to surface measurements [8]. Because of the size of the classic sensors, it is impossible to embed them inside a lamination stack. Significant research has been proposed to develop simulation schemes able to return this internal magnetic distribution [9]-[14]. But, local experimental results have never confirmed the behavior of these simulations due to current sensor limitations. These models have always been validated by comparison to averaged results.

In order to simulate these complicated electromagnetic devices, homogenization methods are proposed but frequently the simulation of each lamination itself is very complex. In this case, the laminated core is considered as a unique element [11]-[14]. These methods rely on local assumptions about the magnetic behavior of each lamination which are currently impossible to verify experimentally. Krismanic et al. have proposed in [15] a solution to develop a smaller sensor for

immersion in a magnetic stack lamination. This sensor is an assembly of a miniaturized 1 mm thick needle sensor and two 1.6 mm H-coils. Although the total sensor thickness is less than 3 mm, positioning this sensor inside the 0.3 mm thickness laminations magnetic core constitutes significant challenges. The research presented here, intends to bridge this gap by printing the sensing method directly onto the magnetic layer within the stack.

In this study, we developed a non-intrusive printed sensor capable of measuring the local magnetic field distribution and evolution with relatively good accuracy. Conductive ink (CI) and the printed electronic method (PE) have been used to design our magnetic induction sensor. The physical concepts of the sensor are based on the needle probe method [16]-[25]. Because of the limited thickness of the printed layer ($< 25 \mu\text{m}$), the sensor can be placed inside a ferromagnetic lamination stack in a non-intrusive way. The sensor can transmit information about the lamination's magnetic behavior throughout the electromagnetic device's life. Since the needle probe method is a magnetic field directional measurement, by coupling a set of sensors and developing smart electric circuit designs, all local magnetic vector information (amplitude, direction, and orientation) becomes accessible. The already manufactured coating dielectric layer of every electric steel sheet ensures the electric isolation of the sensor and avoids electric contact with non-targeted laminations of the magnetic stack. PMNPM sensors are permanent, robust, and relatively inexpensive. They can also be considered good candidates for micro magnetic nondestructive testing of steel components.

PMNPM is described in detail in the first part of this article. The second part is dedicated to the experimental setup developed for the validation of the PMNPM and the third to the experimental validations. In this last part, we will focus on specific experimental conditions where a gradient of magnetic induction can be found through the laminated magnetic core. We will monitor individually the magnetic state of every lamination using the PMNPM and compare the sum of these local measurements to the average value obtained from a classic surrounding coil. These comparisons serve as a validation of the PMNPM.

II - The printed magnetic needle probe method (PMNPM)

a) The classic magnetic needle probe method

The needle probe method was first described by Werner [16] in 1949, and the first electromagnetic device based on the method was built three years after by Stauffer [17]. The limitations of analog electronics coupled to very weak levels of the sensor signals forced researchers in the field to abandon it at the time. Many years after, encouraged by the huge large performance improvements in analog electronics, Japanese researchers revisited Werner's method for the evaluation of the magnetic flux in a ferromagnetic lamination [19]-[23]. In between these studies, Matsubara & al. [22] demonstrated the importance of having a large ratio of distance between tips compared to material thickness. Enokizono & al. [23] succeeded in the estimation of errors in former rotational flux density measurement in both oriented and non-oriented grain electrical steel sheets. Finally, works by Yamaguchi & al. [19] and Senda & al. [20] and [21] showed through theoretical analysis of the methods that it is possible to identify performance enhancements. They concluded that large improvements can be obtained by adjusting factors such as air flux, local stress, nonhomogeneous materials, structure and nature of the magnetizing process. Macroscopic local magnetic properties (magnetic state, magnetizing skill) of a material can be measured using a large panel of local magnetic characterization sensors. Eddy current testing (ECT) [12], [24] and [25], magnetic Barkhausen noise (MBN) [26]-[28], magnetic incremental permeability (MIP) [29]-[32], eddy current magnetic signature (EC-MS) [33] represent some of the measurements used. Although these methods seem to exhibit complementary features, they are all affected by the bulkiness of the sensor design, orientation and position. When viewing this from a non-destructive analysis perspective, this makes it impossible to precisely localize a potential microstructural defect or a residual stress orientation. In general, with these methods, an anisotropic magnetic behavior is very complex to detect. The needle probe method setup tackles this issue by using two needle contacts to build a half-cross sectional coil. The needle probe method provides a well-defined directional measurement which once processed gives a fine image of the local vector magnetic induction field. More precisely, the needle probe method consists of the application

of two probe needles to a ferromagnetic material conductive sheet, forming two point contacts. Based on the potential difference produced by eddy currents generated by ac magnetization, it is possible to measure the flux density in the surrounding area using points 1-2-3-4 as depicted in Fig. 1.

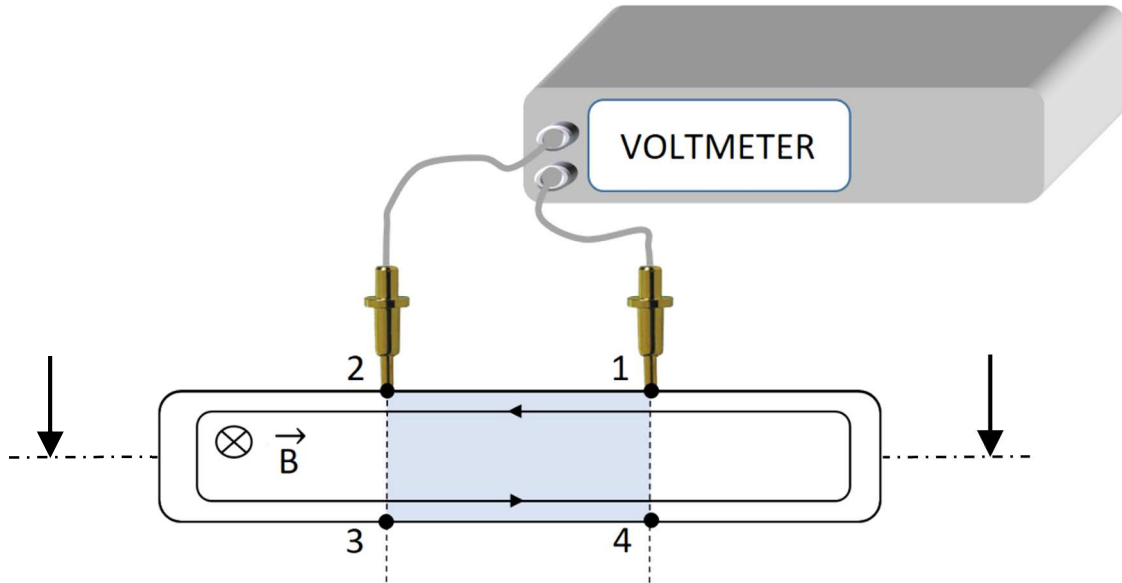


Fig. 1 – Double needle probe method, explanation scheme.

As described in detail in [34], the voltage drop between position 1 and 2 can be approximated to:

$$V_{12} \approx \frac{1}{2} \int_{S_{1234}} \frac{\partial \vec{B}_{1234}}{\partial t} \cdot d\vec{S}_{1234} \quad (1)$$

Where V_{12} is the voltage drop between position 1 and 2. B_{1234} and S_{1234} are respectively the homogeneous magnetic field and the cross section through the position 1234 (Fig. 1).

b) The printed magnetic needle probe method

Printed electronics (PE) is defined as a set of ink based printing methods used to create electrical devices on various substrates. PE has recently emerged as one of the key technologies, from electronics for electrically controlled machines and equipment [35][36]. By combining manufactured electronics to text/graphic prints one can obtain high-quality electric devices with outstanding properties including ultra-thin thicknesses, flexible, wearable, ultra-light, varying geometry, and low cost. PE is particularly attractive because of the possibility of preparing stacks of thin layers (thin-film devices) in a much simpler and cost effective way compared to conventional electronics [37]. The ability to

implement new or improved functionalities is also of major interest. The recent progress of PE is mainly due to improvements in printing technologies but also due to the development of new materials including a variety of conductive inks (CI). CI materials are typically created by infusing graphite or other conductive particles like silver, copper, gold or others in an ink base. Silver inks are now used in everyday applications including printing RFIDs, transit tickets, and printed circuit boards [38]. In this study, the CI and the PE methods have been used to print the needle probes on the surface of a magnetic lamination. The two experimental methods described hereafter have been tested with success to print the sensor.

Mask Method:

The mask method is the most traditional method employed in PCB design. A mask is used to protect areas of the substrate from placement of trace material during the printing process; thereby only the exposed areas represent the routes of the circuit that will be printed. In this case, the technique will be customized in order to prevent alteration of the properties of the substrate which is an electrical steel sheet in our case. That said, a mask is shaped using Graphtec studio software and the cutting plotter CE 6000-40 developed and manufactured by Graphtec Corporation to match the dimensions needed. In this work, 10 mm spacing between the points of contact and a path width of 1mm were used. This is depicted in step 1 of Figure 2. Given that an electrical steel sheet is electrically isolated, step 2 engaged with the mask positioned and fixed on the sheet at the midpoint across the length of the steel sheet in order to avoid edge effects during measurements. At the two points of contact, the insulating coating will be scraped off with care to protect the steel sheet. Step 3 consists of painting a fine layer of silver conductive ink over the mask. This is done using a soft fiber brush in order to prevent damage to the insulating coating found on the sheet. Depending on the type of silver ink: viscosity and the thickness of the path, the drying process may require 10 min at room temperature or an oven to reduce processing time. After curing, the mask is removed and the routes of the sensor remain on the surface of the sheet. Copper tape and twisted electrical wire are attached to the trace for signal collection. Thus, a sensor of approximately 30 microns is achieved and PMPN can be embedded in a

stack of laminations. Fig. 2 below gives an illustration of the different steps required by the “mask” fabrication method.

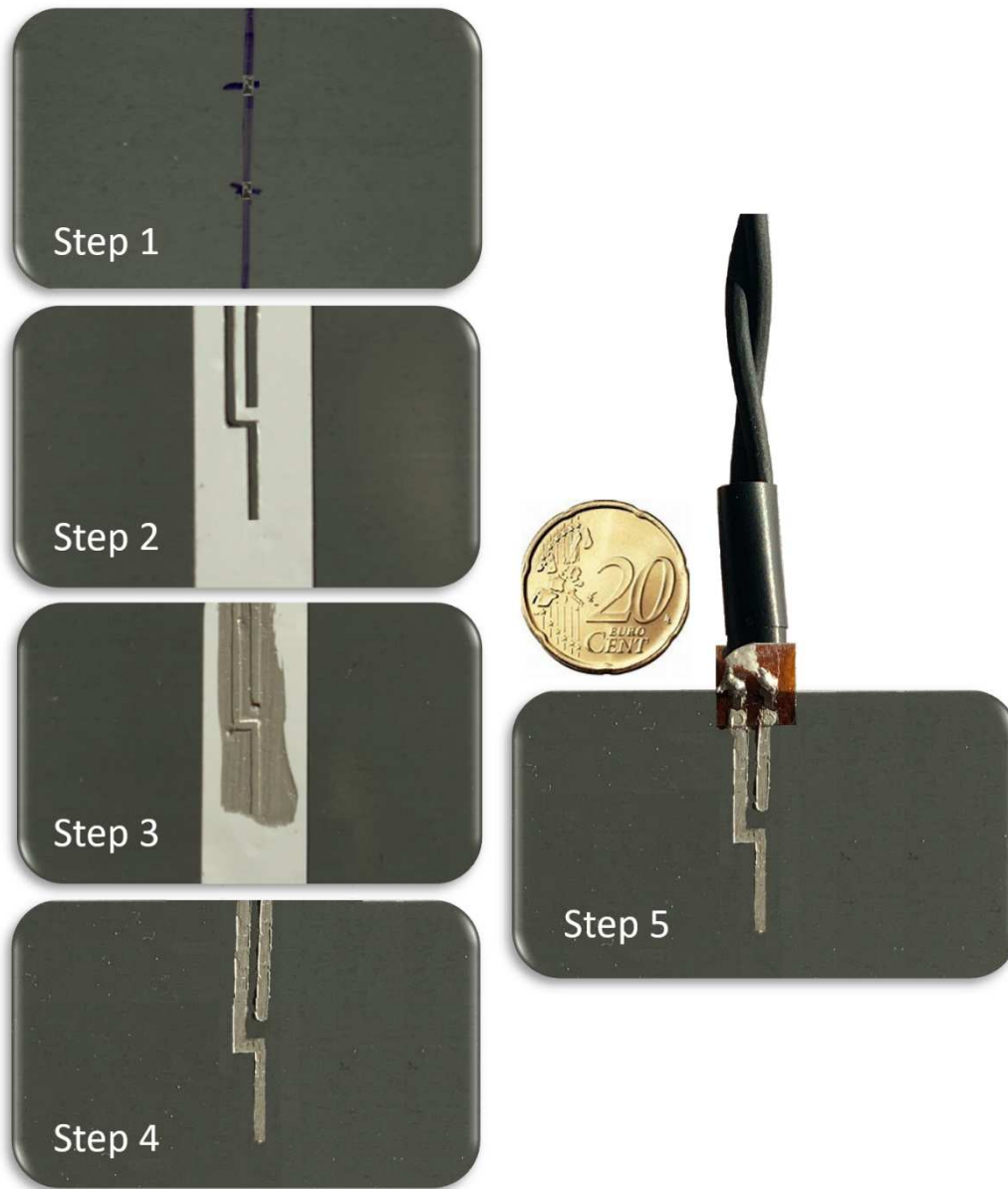


Fig. 2 – PMNPM mask process. Step 1: the coating is removed over the needle contacts. Step 2: the mask is positioned. Step 3: the mask is filled with the silver varnish. Step 4: the mask is removed. Step 5: the electrical connections are established.

Alternatively to this method, a more automatic and sophisticated method of printing is proposed for faster processing and a cleaner layout.

Fabrication with the Sonoplot micro plotter printer:

In order to print sensor traces at the micron level, a high level of control over x-y positioning is required along with control of the volume of ink deposited which controls the thickness of the traces. This was achieved with the aid of a micro plotter instrument (developed by the Sonoplot Company) with an

automatic fluid dispenser (fig. 3). The technique consists initially of filling a dispenser with a 60 micron opening with silver ink. The dispenser which is attached to a piezoelectric material is then vibrated at an appropriate frequency. Depending on the viscosity and volume of fluid loaded in the dispenser, it is calibrated at an appropriate frequency of vibration and voltage to control the dispersion. The fluid will thereby be dispensed onto the steel sheet following a pattern which must be previously drawn in Sonodraw software and saved. The printing process is completed within 15 mins, and the print is left for the ink to get dry as shown in figure 3 below. Finally, measured signals are collected with twisted cables which are interfaced to the sensors' paths using a copper or silver tape

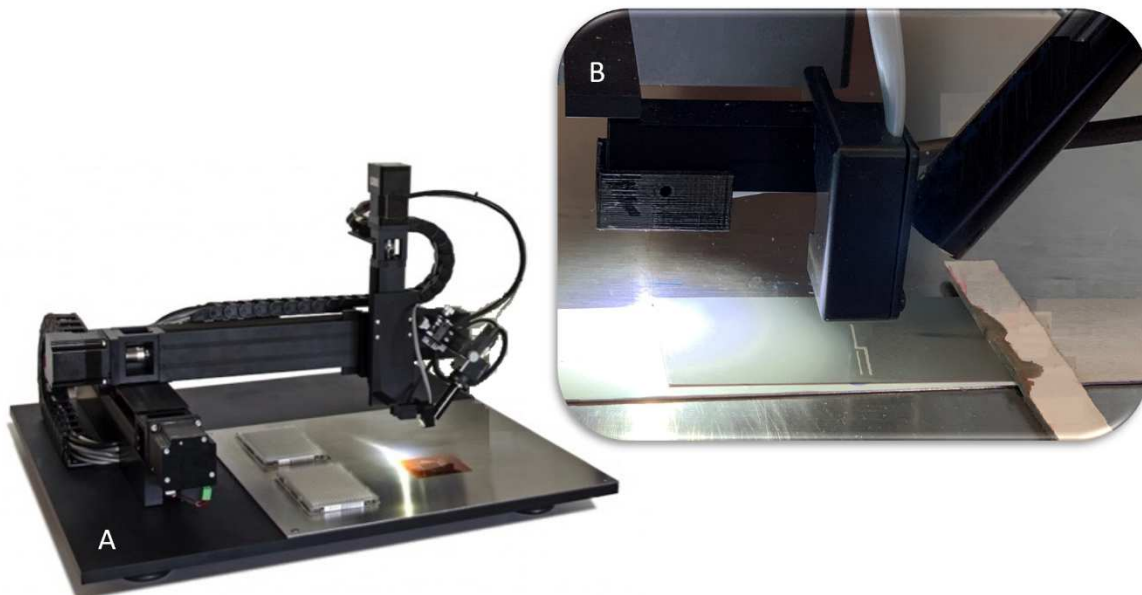


Fig. 3 – a PMNPM Sonoplot printed. 3 – b Zoomed view over the printed area.

A Keyence LJ-V7000 profilometer is used to measure the thickness of the printed circuit. A range of 20 μm to 25 μm is obtained from the Sonoplot method and 24 μm to 28 μm is obtained with the mask method.

III - Experimental setup for the validation of the PMNPM

The overall stacked design of the actual experimental setup used to validate the feasibility of the printed needle probe method is displayed in fig. 4.

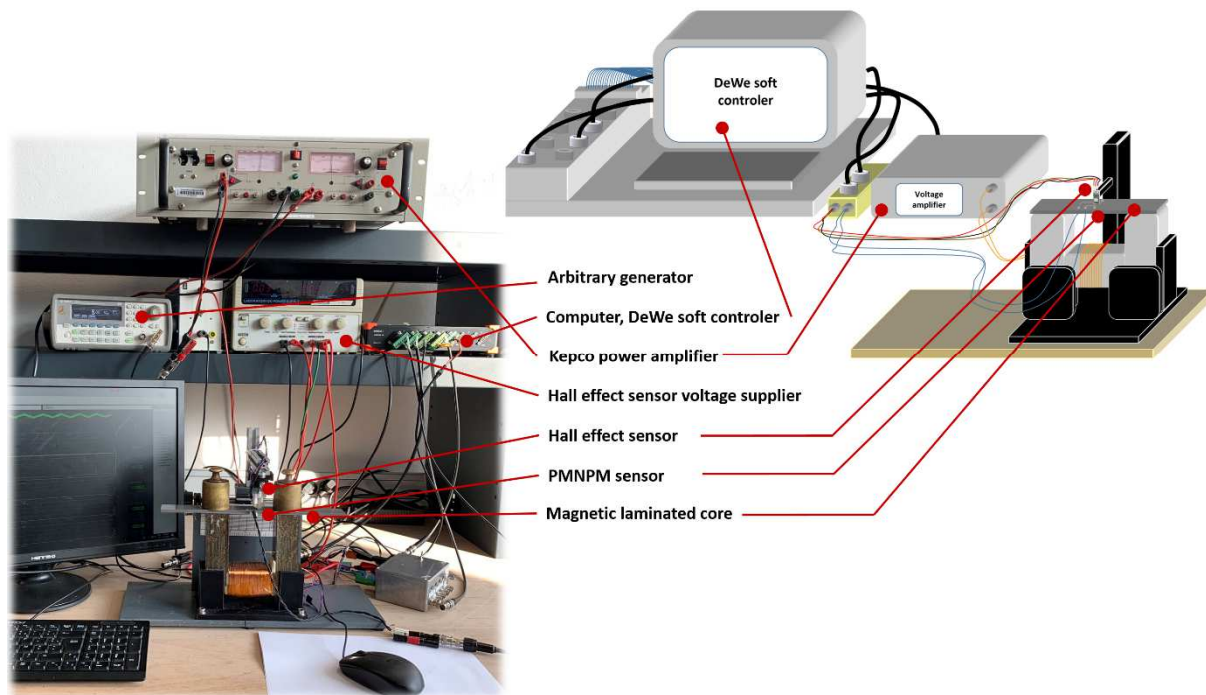


Fig. 4 – 3D Stacked design and photo of the experimental setup.

The single sheet tester standard characterization IEC 60404-3 [39] and [40] has been followed for the development of the experimental characterization bench. This setup is made out of a U-shape yoke, large section ($37 \times 36 \text{ mm}^2$), Fe-Si oriented grains laminated magnetic core. This yoke is surrounded by a 500 turns excitation coil. A power amplifier Kepco BOP 100-4M in its imposed current configuration and driven by a frequency generator Agilent 32220A ensures the coils' electrical energy supply. A noise shielded radiometric linear Hall probe (SS94A from Honeywell) is positioned on top of the tested sample, ideally just in the middle of the needle probe/magnetic sample electric contacts. This sensor measures the surface magnetic field H_{surf} over the probe area. The data-acquisition of both the printed needle probe and the hall sensor voltages is ensured from the DEWESoftX2 data acquisition software associated to a SIRIUSif 8×CAN data acquisition [41]. Numerical integration is performed in post-processing using Matlab™ software. A numerical post processing step correction is also performed to remove the drift due to the integration step. Finally, before each new acquisition, the reproducibility of the results is ensured by a complete demagnetization of the tested sample. The same experimental setup is used for this operation. The excitation coils are subjected to an exponentially decreasing periodic triangular voltage signal. The frequency of the triangular voltage is 50 Hz and a complete

demagnetization lasts approximately 2 minutes. The reproducibility of the experimental results is ensured by repeating each test at least 3-times per experimental test.

a) Isolated magnetic lamination

In the configuration “isolated magnetic lamination”, the monitored lamination is positioned on top of the single sheet tester yoke. To validate the PMNPM, a 10-turns surrounding coil is positioned right next to the printed sensor. Two holes are drilled through the lamination to allow for search coil deployment. The classic needle probe method is tested as well thanks to the classic setup [41]. The tested lamination and sensors are depicted in Figure 5 below. In this configuration, two 0.5 kg weight spacers are positioned on top of the tested sample to limit the air gaps and ensure reproducibility (see fig. 4 and fig. 6).

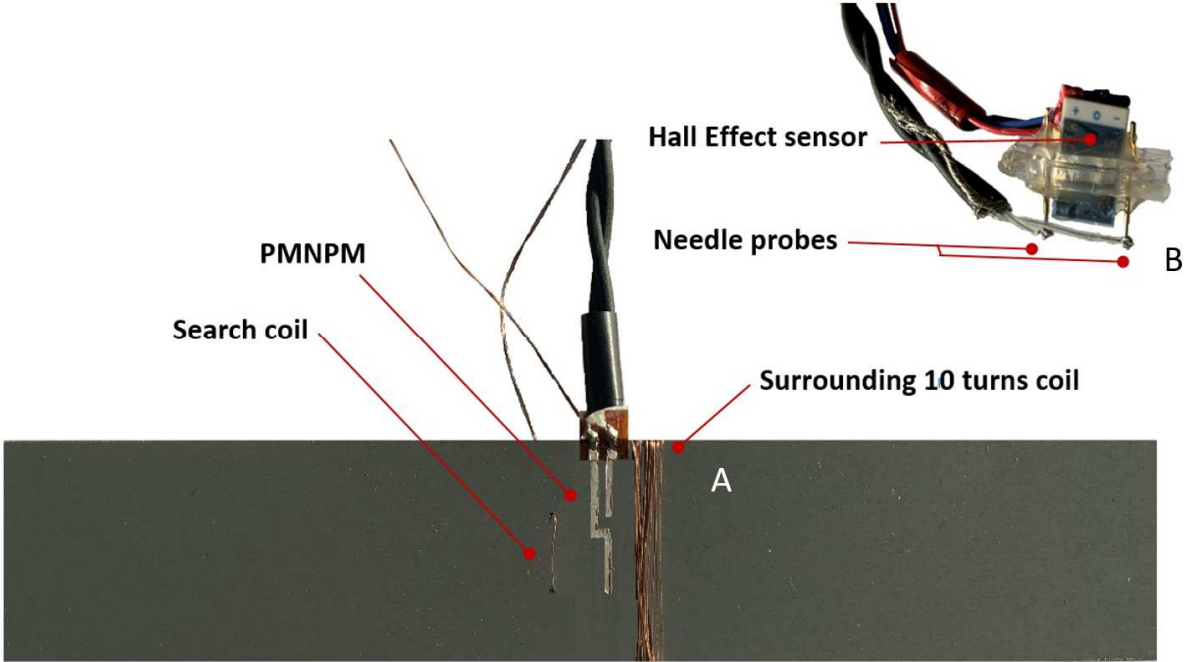


Fig. 5 – a Sensors deployment under isolated magnetic lamination situation. 5 – b Classic needle probe sensor.

b) Laminated magnetic core

In the configuration named “Laminated magnetic core”, a stack of 16 magnetic laminations are positioned on top of the single sheet tester yoke. An instrumented lamination with the printed sensor is positioned successively on every position of the laminated magnetic core (see fig. 6). A 10-turns

surrounding coil can be positioned over the whole magnetic core for the comparison with the sum of the local measurements. A Hall Effect sensor was positioned on the top (H_{TOP}) and on the bottom (H_{BOT}) of the magnetic stack to measure the top and the bottom tangent surface excitation field H . The frequency generator voltage was adjusted for every measurement to maintain the excitation field maximum value as constant as possible.

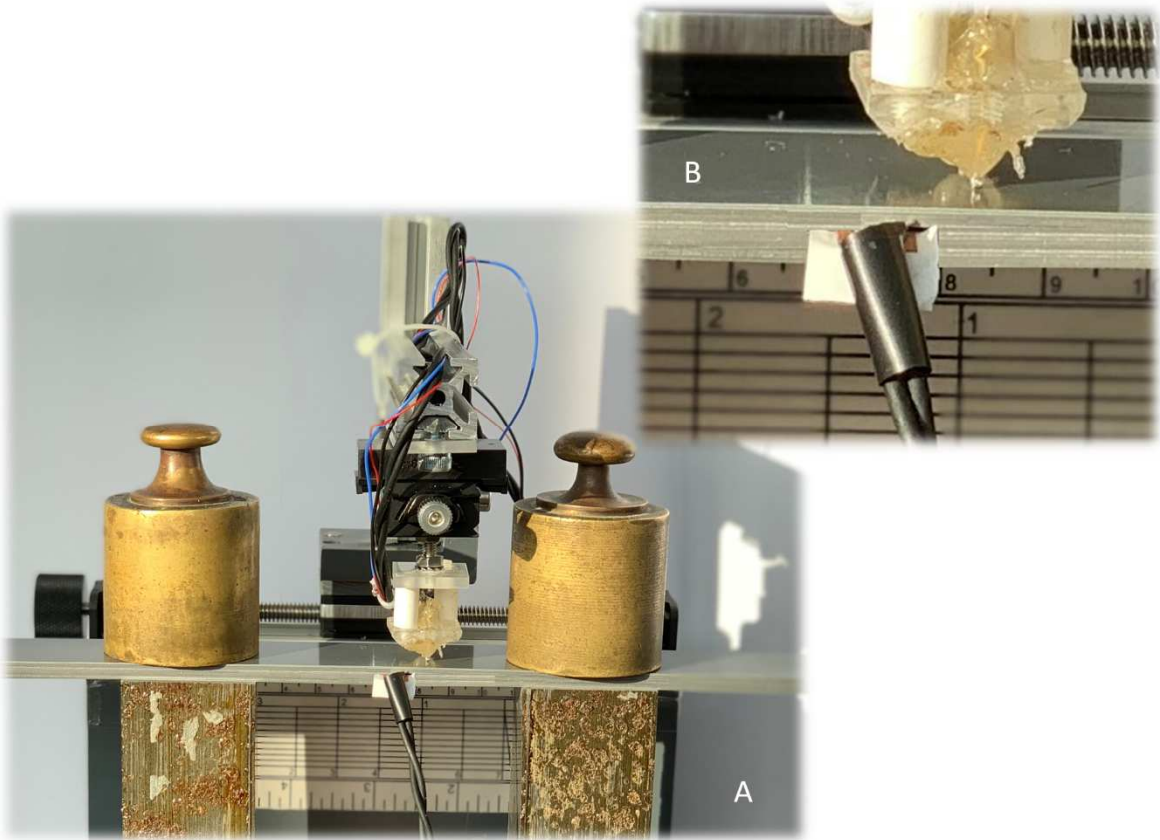


Fig. 6 – a Laminated magnetic core including PMNPM sensor. 6 – b Zoomed view over the sensor area.

IV - Experimental Validation

All the experimental tests have been performed using the experimental setup described in the previous section and from the same magnetic lamination batch. All samples are 0.35 mm thickness with classically oriented grain FeSi laminations with a 3wt% silicon content. Tab. 1 provides typical values for room temperature FeSi GO basic magnetic parameters.

Tab. 1 – Typical values of FeSi GO basic magnetic parameters at room temperature.

	Composition	Max. relative permeability (μ_{max})	Coercive field H_c (A/m)	Saturation polarization J_s (T)	Curie Temperature T_c (°C)	Saturation magnetostriction $\lambda_s=(\Delta l/l)_s$
GO Fe-Si	Fe ₉₇ -Si ₃	15 - 80 x 10 ³	4 - 15	2.02	750	1 - 3 x 10 ⁻⁶

As previously described, a varnish coating is applied during stack manufacturing. The coating provides electrical isolation. This specific magnetic lamination material has been chosen for several reasons:

- It is one of the most common magnetic material grades used as electric steel.
- The magnetic properties are relatively homogenous in the standard frequency range.
- It is highly anisotropic which is a property that should be measured during testing.

a) Isolated magnetic lamination

The first experimental situation tested is the configuration “isolated magnetic lamination” described in Section III - a. Initial results show the hysteresis cycles obtained with the four sensors (PMNPM, classic needle probe, 10 turns surrounding coil and search coil). In this first case, the magnetic excitation field has a parallel direction to the magnetic easy axis. The frequencies tested ranged from 1 Hz to 200 Hz.

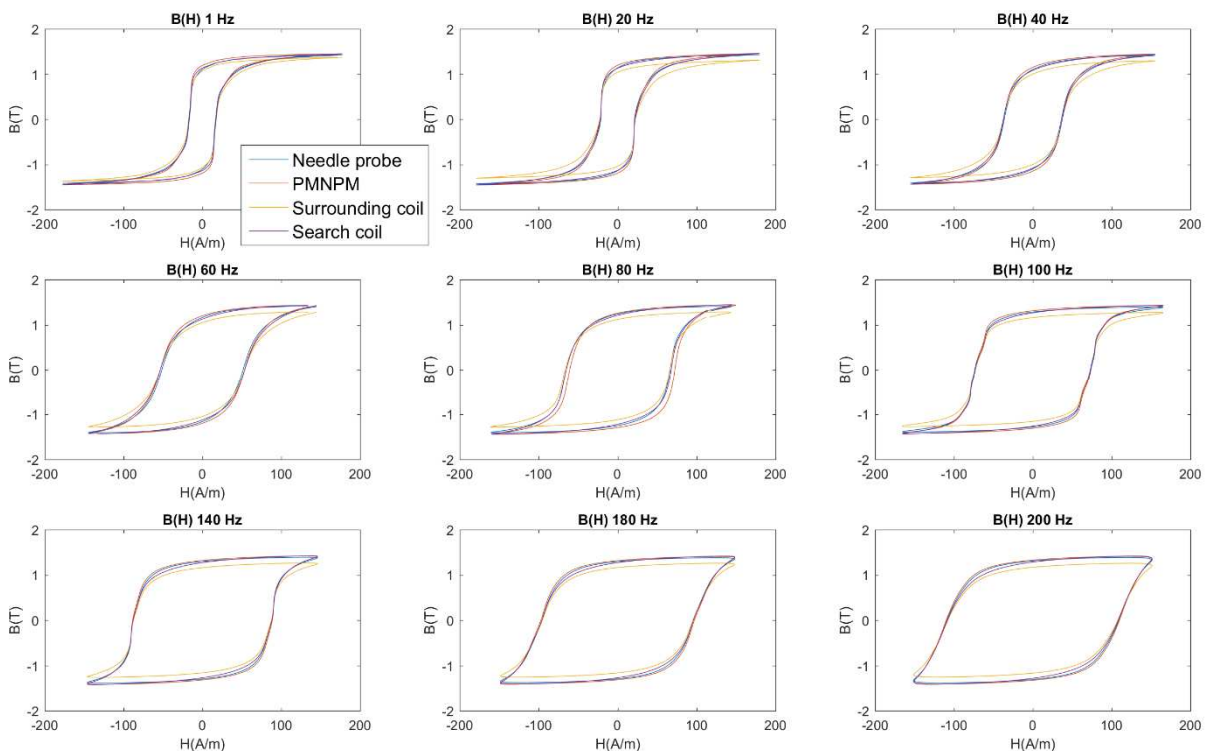


Fig. 7 – Hysteresis cycles obtained under isolated magnetic lamination situation and for increasing frequency levels.

For all the frequencies tested, successful measurements were observed. Small differences were noticed between the amplitude of the magnetic induction measured with the surrounding coil and the

amplitudes measured with the other sensors. This difference is possibly due to edge effects and non-homogeneous behaviors coming from the manufacturing processes or unexpected asymmetrical properties of the experimental setup.

For the results presented in the next figure (fig. 8), the same material, the same sensors and the same frequencies were tested. The direction of the magnetic excitation field was now perpendicular to the magnetic easy axis. Results showed unusual but classic results under such conditions depicting hysteresis cycles with sigmoid shapes including two high permeability areas.

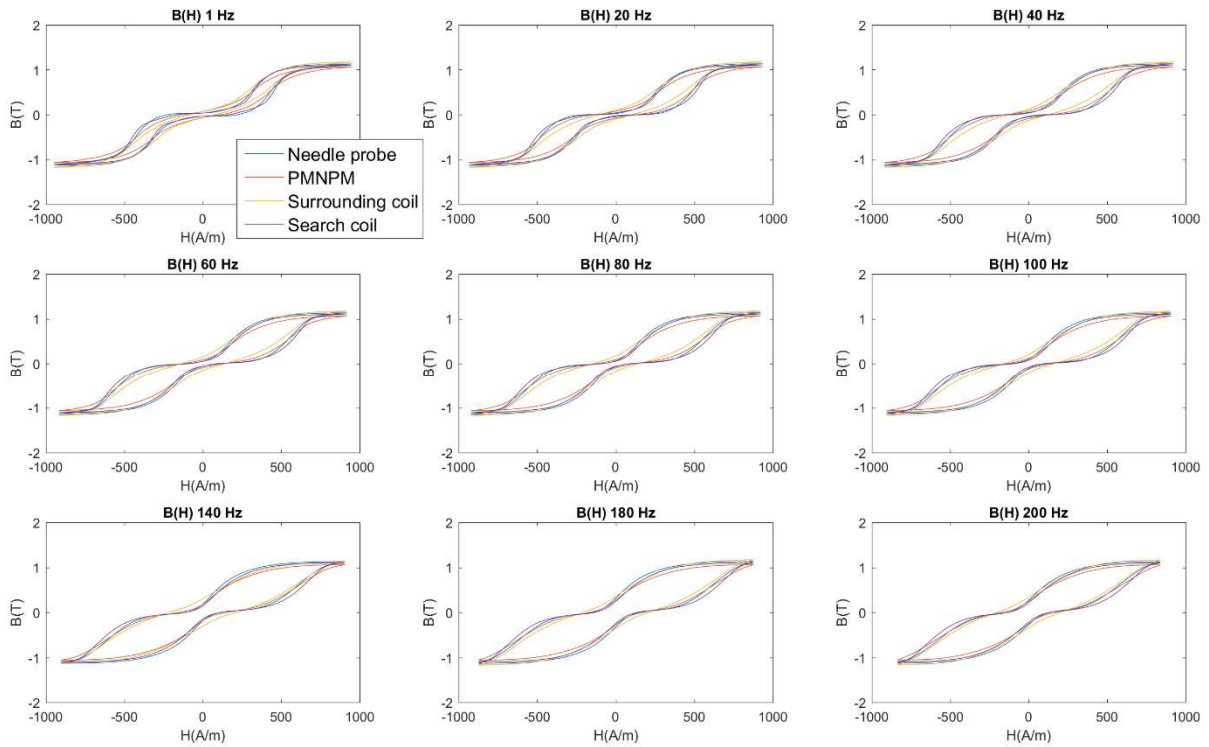


Fig. 8 – Hysteresis cycles obtained under isolated magnetic lamination situation and for increasing frequency levels.

These results depict expected results for both experimental configurations. According to the standard for the single sheet tester characterization [39], a surrounding coil is the conventional sensor. By calculating and comparing the hysteresis areas as proposed in Tab. 2 and 3, the precision of the new sensor can be established. The Error functions are calculated from the following equations:

$$\begin{cases} Error_{coil}(\%) = 100 \cdot \left(1 - abs \left(\frac{\langle A \rangle_{PMNPM}}{\langle A \rangle_{Coil}} \right) \right) \\ Error_{S.coil}(\%) = 100 \cdot \left(1 - abs \left(\frac{\langle A \rangle_{PMNPM}}{\langle A \rangle_{S.Coil}} \right) \right) \end{cases} \quad (2)$$

Tab. 2 – Precision of the PMNPM sensor compared to the conventional one (coil and search coil) under easy axis magnetic excitation situation.

		1 Hz	20 Hz	40 Hz	60 Hz	80 Hz	100 Hz	140 Hz	180 Hz	200 Hz
Easy axis direction	Hysteresis Area PMNPM (J/m^3)	111,85	142,97	190,80	255,61	287,75	383,65	451,33	500,74	558,70
	Hysteresis Area coil (J/m^3)	113,19	140,87	183,96	242,92	263,51	351,63	403,16	447,10	494,82
	Hysteresis Area Search Coil (J/m^3)	114,99	146,01	196,03	262,95	287,04	382,61	445,58	495,54	549,38
	Error (%) coil comparison	1,19%	1,49%	3,71%	5,22%	9,20%	9,11%	11,95%	12,00%	12,91%
	Error (%) search coil comparison	2,81%	2,13%	2,74%	2,87%	0,24%	0,27%	1,27%	1,04%	1,67%

Tab. 3 – Precision of the PMNPM sensor compared to the conventional one (coil and search coil) under transverse magnetic excitation situation.

		1 Hz	20 Hz	40 Hz	60 Hz	80 Hz	100 Hz	140 Hz	180 Hz	200 Hz
Transverse direction	Hysteresis Area PMNPM (J/m^3)	309,41	471,79	599,32	709,01	777,72	846,40	942,98	917,07	1048,69
	Hysteresis Area coil (J/m^3)	260,85	417,15	530,06	634,39	699,29	754,06	867,12	902,13	970,82
	Hysteresis Area Search Coil (J/m^3)	293,07	464,22	589,76	688,53	754,16	811,67	929,04	912,68	1019,53
	Error (%) coil comparison	18,62%	13,10%	13,07%	11,76%	11,22%	12,25%	8,75%	1,66%	8,02%
	Error (%) search coil comparison	5,28%	1,61%	1,59%	2,89%	3,03%	4,10%	1,48%	0,48%	2,78%

From the observation of both Tab. 2 and 3, one can conclude the PMNPM sensor shows high accuracy. The small divergences observed through the comparisons with the surrounding coil are probably due to some edges inhomogeneity coming from the lamination building process.

b) Laminated magnetic core

The next set of results come from the second experimental situation: “laminated magnetic core” configuration as described in III – b. In Fig. 9 below, we plotted the magnetic induction state measured locally for every lamination of the laminated magnetic core as a function of the tangent excitation field measured simultaneously on the laminations stack top and bottom. Lamination 1 is positioned directly in contact with the yoke of the single sheet tester, lamination 16 is set at the opposite position of the magnetic core (see Fig. 10 – d). The magnetic excitation field has a parallel direction to the magnetic easy axis. The maximum value of the magnetic excitation field is set to be intentionally weak to create a strong gradient of magnetic induction through the laminated magnetic core. As illustrated in Fig. 9 and 10 – a, the maximum magnitude of the magnetic induction field decreases exponentially with the distance of the single sheet tester inductor. A similar trend can be observed for the evolution of the

hysteresis losses (Fig. 10 – b). The absolute value of the coercive fields (Fig. 10 – c) are linearly slowly decreasing.

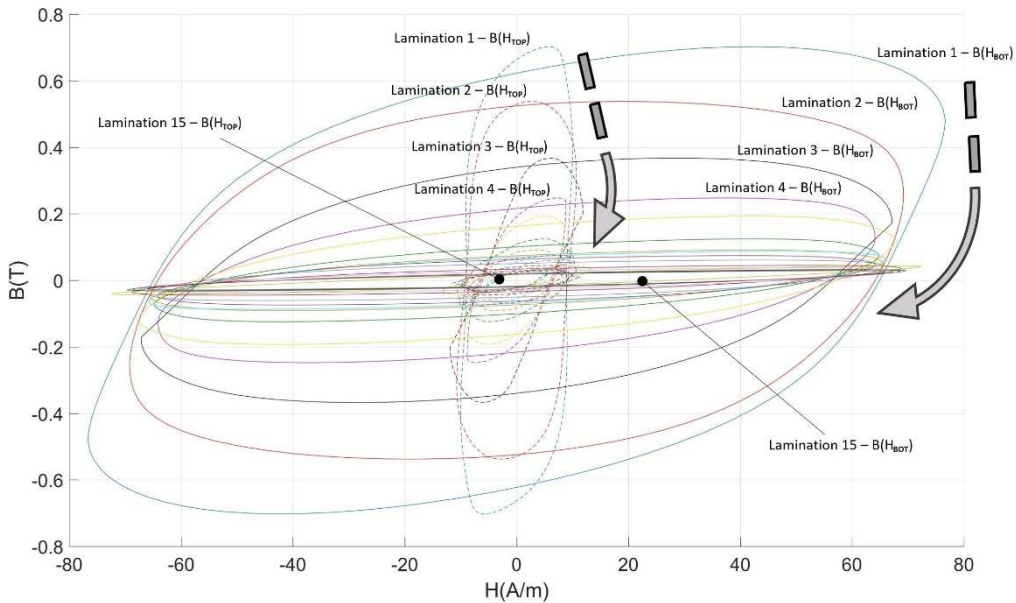


Fig. 9 – Hysteresis cycles obtained under isolated magnetic lamination situation and for increasing frequency levels.

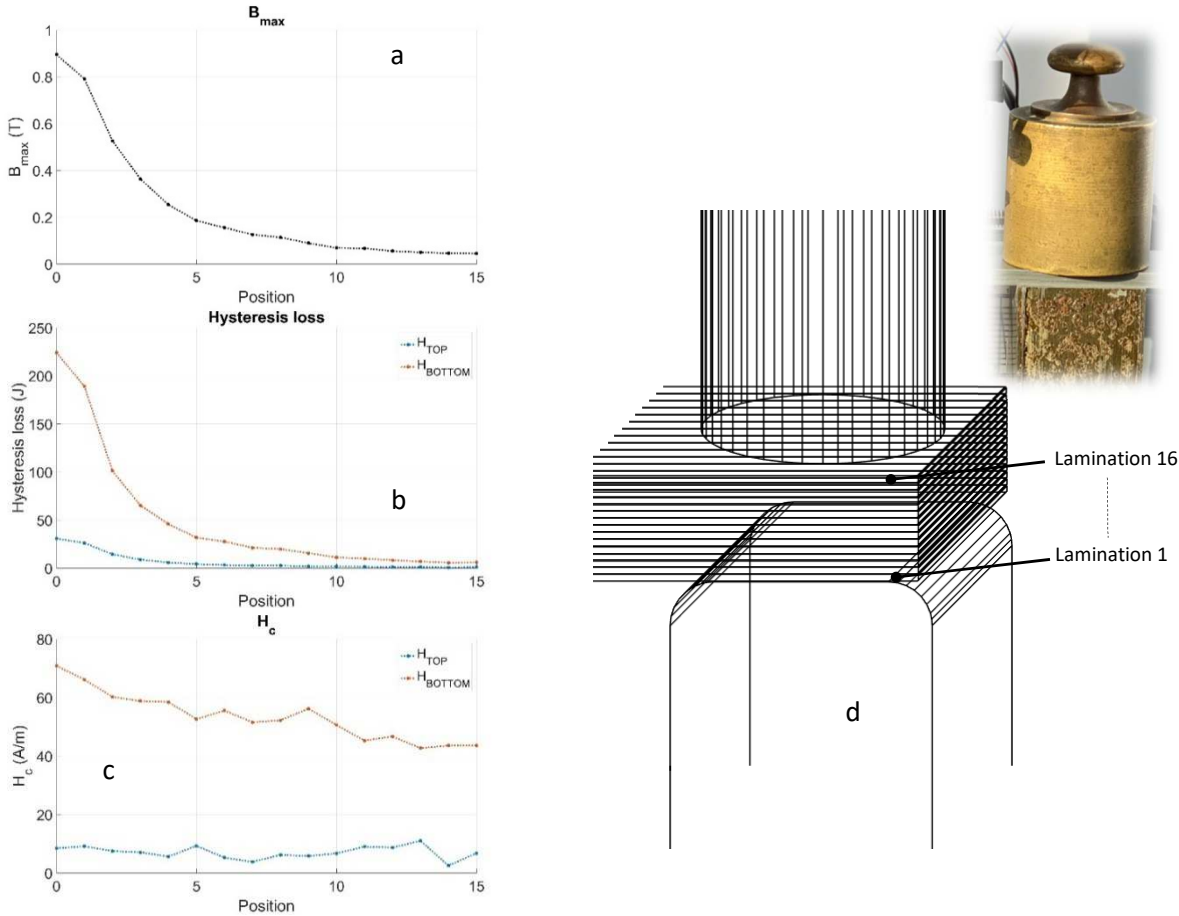


Fig. 10 – a Maximal induction field versus lamination position, 10 – b Hysteresis losses versus lamination position, 10 – c Coercivity versus lamination position, 10 – d Illustration of the lamination position.

Finally, a validation of the PMNPM is proposed by comparing reconstructed hysteresis cycles from local measurements to the one obtained with the 10-turns surrounding coil positioned over the whole magnetic core. The average induction state is obtained through the conservation of the magnetic flux:

$$\begin{aligned}\phi_{tot} &= \sum_{i=1}^{16} \phi_i \\ B_{tot} \cdot S_{tot} &= \sum_{i=1}^{16} B_i \cdot S_i \quad S_{tot} = 16 \cdot S_i \\ B_{tot} &= \frac{1}{16} \sum_{i=1}^{16} B_i\end{aligned}\tag{2}$$

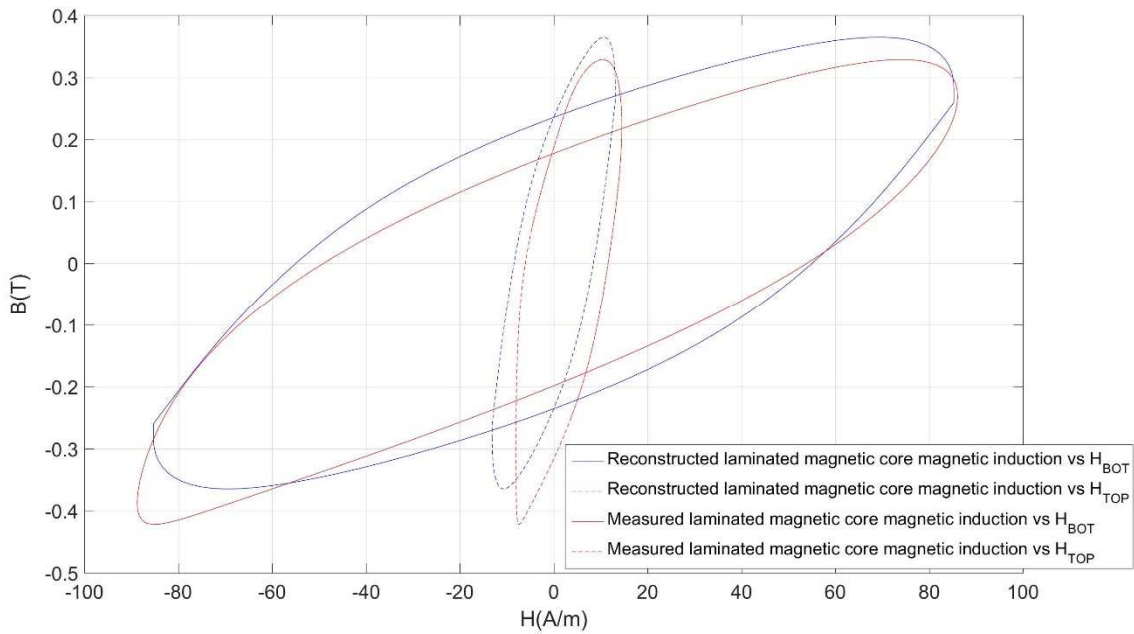


Fig. 11 – Comparisons between the reconstructed laminated hysteresis cycles and the measured ones.

Figure 11 depicts highly comparable curves for both H_{BOT} and H_{TOP} reconstructed hysteresis cycles and the experimental cycles proving the validity of the needle probes method. These results provide evidence for the feasibility of monitoring isolated magnetic lamination states through the laminated magnetic core. By comparing the surface areas between the measured and the reconstructed hysteresis cycles, the error obtained under H_{BOT} is 13.5%, and just 2.1% for the H_{TOP} cases.

V - Conclusion

This work demonstrated that by using a uniform magnetization model, the voltage detected by the needle probes method is almost equivalent to values measured using a classic search coil (one turn) wound around the 1-2-3-4 area as seen in fig 1. It is stated that when the span between probes is about 10 mm, it is possible to evaluate with relatively high accuracy localized flux densities in grain-oriented electrical steel sheets. This research demonstrated the problem of the needle technique and improved it with a reduced distance in a non-invasive manner by printing conductive ink directly to the laminate substrate. This method drastically reduces sensor volume and geometrical constraints. Magnetic induction and hysteresis results have been obtained using the printed sensor in frequency ranges of 1 Hz to 200 Hz, confirming this type of sensing can provide information on the internal magnetic behaviour of a magnetic lamination stack. PMNPM can be incorporated into the manufacturing process for continual health monitoring of electric steel components or it can be used as a continuous tool for structural health monitoring of bearings, gear boxes, bridges and buildings. As the magnetic behaviour is highly dependent on the internal mechanical properties, such continuous magnetic monitoring can be used to predict and prevent macroscopic failures and potential catastrophes.

References:

- [1] M. Vazquez and A. Hernando, "A soft magnetic wire for sensor applications", *J. of Phys. D: App. Phys.*, vol. 29, n°4, pp. 939-949, 1996.
- [2] B. Nick, "Laminated magnetic core for use in an electric inductive device", *US Pat.* 3, 122, 667, 1964.
- [3] R.H. Pry, C.P. Bean, "Calculation of the energy loss in magnetic sheet materials using a domain model", *J. of App. Phys.*, vol. 29, iss. 532, 1958.
- [4] B. Ducharne, G. Sebald, D. Guyomar, G. Litak, "Dynamics of magnetic field penetration into soft ferromagnets", *J. of App. Phys.*, pp. 243907, 2015.
- [5] Electrical Steel Market by Type (Grain-oriented and Non-Grain-oriented), Application (Transformers, Motors, Inductors), End-Use Industry (Energy, Automobile, Manufacturing, Household Appliances), and Region - Global Forecast to 2021, Market research report, 2017.
- [6] The world databank
- [7] Beatty, *Standard Handbook for Electrical Engineers* 11th ed., pg. 4-111
- [8] J.R. Sheats, *Journal of Materials Research* 2004; 19 1974.
- [9] S. Tumanski, "Induction coil sensors – a review", *Meas. Sci. Technol.*, vol. 18, R31-R46, 2007.
- [10] J.P.A. Bastos, N. Sadowski, "Electromagnetic modeling by finite element methods", Marcel Dekker Inc., New-York, 2003.
- [11] F. Piriou, A. Razek, "Finite element analysis in electromagnetic systems-accounting for electric circuits", *IEEE Trans. on Mag.*, vol. 29, iss. 2, 1993.
- [12] B. Gupta, B. Ducharne, G. Sebald, T. Uchimoto, "A space discretized ferromagnetic model for non-destructive eddy current evaluation", *IEEE Trans. on. Mag*, vol. 54 Iss. 3, 2018.
- [13] M. A. Raulet, B. Ducharne, J.P. Masson, and G. Bayada, "The magnetic field diffusion equation including dynamic hysteresis: a linear formulation of the problem", *IEEE Trans. on Mag.*, vol. 40, n° 2, pp. 872 – 875, 2004.
- [14] B. Ducharne, G. Sebald, D. Guyomar, G. Litak, "Fractional model of magnetic field penetration into a toroidal soft ferromagnetic sample", *Int. J. of Dyn. And Cont.*, pp. 1-8, 2017.
- [15] G. Krismanic, H. Pfützner, N. Baumgartinger, "A hand-held sensor for analyses of local distribution of magnetic fields and losses", *J. of Mag. and Mag. Mat.*, vol. 215-216, pp. 720-722, 2000.
- [16] E. Werner, *Austrian Patent* n° 191015, 1949.
- [17] L. H. Stauffer, *U.S.A. Patent* No 2828467, 1952.
- [18] W. Salz and K. A. Hempel, "Which field sensors are suitable for a rotating flux apparatus?," in *Int. Workshop on Mag. Prop. of Elec. Steel Sheet Under 2-D Excitation*, 1992.
- [19] T. Yamaguchi, K. Senda, M. Ishida, K. Sato, A. Honda and T. Yamamoto, 'Theoretical analysis of localized magnetic flux measurement by needle probe', *J. Physique IV*, 8 717–20 Pr2, 1998.
- [20] K. Senda, M. Ishida, K. Sato, M. Komatsubara and T. Yamaguchi, 'Localized magnetic properties in grain-oriented silicon steel measured by stylus probe method', *Trans. IEEE Japan*, pp. 941–50, 1997.

- [21] K. Senda, M. Ishida, K. Sato, M. Komatsubara and T. Yamaguchi, 'Localized magnetic properties in grain-oriented electrical steel measured by needle probe method', *Electr. Eng. Japan*, 126 942–9, 1999.
- [22] K. Matsubara, T. Nakata, and Y. Kadota, "A novel method of measurements of magnetic flux in silicon steel sheet with magnetic flux leakage," in *National Conf IEE Japan*, 1988, 1665.
- [23] M. Enokizono and I. Tanabe, "The problem of simplified two dimensional magnetic measurement apparatus," in *5th International Workshop on 1 and 2-Dimensional Magnetic Measurement and Testing*, 1999.
- [24] J. Garcia-Martin, J. Gomez-Gil, E. Vasquez-Sanchez, "Non-destructive techniques based on eddy current testing", *Sensors*, vol. 11, iss. 3, pp. 2525-2565, 2011.
- [25] S. Yamada, M. Katou, M. Iwahara, F.P. Dawson, "Eddy current testing probe composed of planar coils", *IEEE Trans. on Mag.*, vol. 31, iss. 6, pp. 3185-3187, 1995.
- [26] B. Ducharne, B. Gupta, Y. Hebrard, J. B. Coudert, "Phenomenological model of Barkhausen noise under mechanical and magnetic excitations", *IEEE Trans. on. Mag*, vol. 99, pp. 1-6, 2018.
- [27] T. L. Manh, F. Caleyó, J.M. Hallen, J.H. Espina-Hernández, J.A. Pérez-benitez, "Model for the correlation between magnetocrystalline energy and Barkhausen noise in ferromagnetic materials", *J. of Mag. and Mag. Mat.*, vol. 454, pp. 155-164, 2018.
- [28] B. Ducharne, MQ. Le, G. Sebald, PJ. Cottinet, D. Guyomar, Y. Hebrard, "Characterization and modeling of magnetic domain wall dynamics using reconstituted hysteresis loops from Barkhausen noise", *J. of Mag. And Mag. Mat.*, pp. 231-238, 2017.
- [29] A.Yashan, G.Dobmann, "Measurements and Semi-analytical modeling of incremental permeability using eddy current coil in the presence of magnetic hysteresis", *Studies Appl. Electromag. Mech.*, vol. 23, pp. 150–157, 2002.
- [30] G.Dobmann, "Physical basics and industrial application of 3MA-micromagnetic multiparameter microstructure and stress analysis", *Studies Appl. Electromag. Mech.*, vol. 31, pp. 18–25, 2008.
- [31] B. Gupta, B. Ducharne, T. Uchimoto, G. Sebald, T. Miyazaki, T. Takagi, "Physical Interpretation of the Microstructure for aged 12 Cr-Mo-V-W Steel Creep Test Samples based on Simulation of Magnetic Incremental Permeability", *J. of Mag. and Mag. Mat.*, vol. 486, 2019.
- [32] B. Gupta, T. Uchimoto, B. Ducharne, G. Sebald, T. Miyazaki, T. Takagi, "Magnetic incremental permeability non-destructive evaluation of 12 Cr-Mo-W-V Steel creep test samples with varied ageing levels and thermal treatments", *NDT & E Int.*, accepted for publication, 2019.
- [33] T. Matsumoto, T. Uchimoto, T. Takagi, G. Dobmann, B. Ducharne, S. Oozono, H. Yuya, "Investigation of Electromagnetic Nondestructive Evaluation of Residual Strain in Low Carbon Steels Using the Eddy Current Magnetic Signature (EC-MS) Method", *J. of Mag. And Mag. Mat.*, vol. 479, pp. 212-221, 2019.
- [34] G. Loisos, A.J. Moses, "Critical Evaluation and limitations of Localized flux density measurements in electrical steels", *IEEE Trans. on Mag.*, vol. 37, n°4, pp. 2755-2757, 2001.
- [35] J. Perelaer, P.J. Smith, D. Mager, D. Soltman, S.K. Volkman, V. Subramanian, J.G. Korvink, U.S. Schubert, "Printed electronics: the challenges involved in printing devices, interconnects, and contacts based on inorganic materials", *J. Mater. Chem.*, vol. 20, pp. 8446-8453, 2010.

- [36] M. Berggren, D. Nilsson, N.D. Robinson, "Organic materials for printed electronics", *nature materials*, vol. 6, pp. 3-5, 2007.
- [37] J.R. Sheats, "Manufacturing and commercialization issues in organic electronics", *J. of Materials Research*, vol. 19, iss. 7, pp. 1974-1989, 2004.
- [38] B. K. Park, D. Kim, S. Jeong, J. Moon, J.S. Kim, "Direct writing of copper conductive patterns by ink-jet printing", *Thin solid films*, vol. 515, iss. 19, pp. 7706-7711, 2007.
- [39] "Methods of measurement of the magnetic properties of electrical steel strip and sheet by means of a single sheet tester", *International Standard IEC 60404-3*, 2002.
- [40] "Guide for measuring power frequency magnetic properties of flat-rolled electrical steels using small single sheet testers", *ASTM International Tech. Rep. A1036*, 2009.
- [41] Y.A. Tene Deffo, P. Tsafack, B. Ducharme, B. Gupta, A. Chazotte-Leconte, L. Morel, "Local measurement of peening-induced residual stresses on Iron Nickel material using needle probes technique", *IEEE Trans on Mag.*, 2019.